Exploring time like tranistions in pp, πp and AA reactions with HADES

Piotr Salabura for the HADES collaboration[3,*]
and J. Adamczewski-Musch[4], B. Arnoldi-Meadows[8], A. Belounnas[16], A. Belyaev[7],A. Blanco[1], C. Blume[8], M. Böhmer[10], S Borisenko[13], L. Chlad[17], P. Chudoba[17], I. Ciepał[2], D. Dittert[5], J. Dreyer[6], W. Esmail[12], M. Dürr[11], L. Fabbietti[10,9], O. Fateev[7], P. Fonte[1,a], J. Friese[10], I. Fröhlich[8], J. Förtsch[19], T. Galatyuk[5,4], R. Gernhäuser[10], O. Golosov[15], M. Golubeva[13], R. Greifenhagen[6,b], F. Guber[13], M. Gumberidze[4], S. Harabasz[5,3], R. Hensch[8], C. Höhne[11,4], R. Holzmann[4], H. Huck[8], A. Ierusalimov[7], A. Ivashkin[13], B. Kämpfer[6,b], K-H. Kampert[19], B. Kardan[8], I. Koenig[4], W. Koenig[4], G. Kornakov[5], F. Kornas[5], R. Kotte[6], A. Kozela[2], I. Kres[19], J. Kuboś[2], A. Kugler[17], P. Kulesa[12], V. Ladygin[7], R. Lalik[3], A. Lebedev[14], S. Lebedev[11,7], S. Linev[4], L. Lopes[1], M. Lorenz[8], G. Lykasov[7], T. Mahmoud[11], A. Malige[3], J. Markert[4], T. Matulewicz[18], S. Maurus[10], V. Metag[11], J. Michel[8], S. Morozov[13,15], C. Müntz[8], L. Naumann[6], K. Nowakowski[3], J.-H. Otto[11], V. Patel[19], C. Pauly[19], V. Pechenov[4], O. Pechenova[4], O. Petukhov[13], D. Pfeifer[19], K. Piasecki[18], J. Pietraszko[4], A. Prozorov[17], W. Przygoda[3], K. Pysz[2], B. Ramstein[16], N. Rathod[3], A. Reshetin[13], L. Ritman[12], P. Rodriguez-Ramos[17], A. Rost[5], P. Salabura[3], F. Scozzi[5,16], F. Seck[5], I. Selyuzhenkov[4,15], I Shabanov[13], US Singh[3], J. Smyrski[3], S. Spies[8], H. Ströbele[8], J. Stroth[8,4], J. Stumm[8], O. Svoboda[17], M. Szala[8], P. Tlusty[17], M. Traxler[4], C. Ungethüm[5], O. Vazquez-Doce[10,9], V. Wagner[17], A.A. Weber[11], C. Wendisch[4], M.G. Wiebusch[8], P. Wintz[12], J. Wirth[10,9], A. Zhilin[14], P. Zumbruch[4]

[1]LIP-Laboratório de Instrumentação e Física Experimental de Partículas , 3004-516 Coimbra, Portugal
[2]Institute of Nuclear Physics, Polish Academy of Sciences, 31342 Kraków, Poland
[3]Smoluchowski Institute of Physics, Jagiellonian University of Cracow, 30-059 Kraków, Poland
[4]GSI Helmholtzzentrum für Schwerionenforschung GmbH, 64291 Darmstadt, Germany
[5]Technische Universität Darmstadt, 64289 Darmstadt, Germany
[6]Institut für Strahlenphysik, Helmholtz-Zentrum Dresden-Rossendorf, 01314 Dresden, Germany
[7]Joint Institute of Nuclear Research, 141980 Dubna, Russia
[8]Institut für Kernphysik, Goethe-Universität, 60438 Frankfurt, Germany
[9]Excellence Cluster 'Origin and Structure of the Universe' , 85748 Garching, Germany
[10]Physik Department E62, Technische Universität München, 85748 Garching, Germany
[11]II.Physikalisches Institut, Justus Liebig Universität Giessen, 35392 Giessen, Germany
[12]Forschungszentrum Juelich, 52428 Juelich, Germany
[13]Institute for Nuclear Research, Russian Academy of Science, 117312 Moscow, Russia
[14]Institute of Theoretical and Experimental Physics, 117218 Moscow, Russia
[15]National Research Nuclear University MEPhI (Moscow Engineering Physics Institute), 115409 Moscow, Russia
[16]Institut de Physique Nucléaire, CNRS-IN2P3, Univ. Paris-Sud, Université Paris-Saclay, F-91406 Orsay Cedex, France
[17]Nuclear Physics Institute, The Czech Academy of Sciences, 25068 Rez, Czech Republic
[18]Uniwersytet Warszawski - Instytut Fizyki Doświadczalnej, 02-093 Warszawa, Poland
[19]Bergische Universität Wuppertal, 42119 Wuppertal, Germany

[a] also at Coimbra Polytechnic - ISEC, Coimbra, Portugal
[b] also at Technische Universität Dresden, 01062 Dresden, Germany

Abstract. Radiative transition of an excited baryon to a nucleon with emission of a virtual massive photon converting to dielectron pair (Dalitz decays) provides important information about baryon-photon coupling at low q^2 in timelike region. A prominent enhancement in the respective electromagnetic transition Form-Factors (etFF) at q^2 near vector mesons ρ/ω poles has been predicted by various calculations reflecting strong baryon-vector meson couplings. The understanding of these couplings is also of primary importance for the interpretation of the emissivity of QCD matter studied in heavy ion collisions via dilepton emission. Dedicated measurements of baryon Dalitz decays in proton-proton and pion-proton scattering with HADES detector at GSI/FAIR are presented and discussed. The relevance of these studies for the interpretation of results obtained from heavy ion reactions is elucidated on the example of the HADES results.

[*]e-mail: piotr.salabura@uj.edu.pl

1 Introduction

QCD describes nucleons as colorless states of three nearly massless quarks confined to a small volume due to the strong force. The building blocks are light (u,d) quarks with current mass of only a few MeV emerging from the famed Higgs mechanism. Their much larger constituent mass is generated by the coupling of the quarks to the non-trivial QCD vacuum [1]. The underlying mechanism of the light quark mass generation is the spontaneous chiral symmetry breaking which leads to the appearance of Goldstone bosons, identified in the SU(2) flavour symmetry with pions, and chiral parity doublets (for example $\rho - a_1$ or nucleon- $N^*(1535)$) with a large mass difference. The order parameter of the chiral symmetry breaking is the non vanishing expectation value of the quark-anti quark condensate related to the pion decay constant by the Gell-Mann-Oaknes-Renner relation. Various model calculations predict a significant depletion of the expectation value of the quark condensate as a function of the temperature T and baryon-chemical potential μ_b. Lattice calculations performed in the limit of vanishing baryo-chemical potential predict a crossover phase transition from the hadron gas to the quark-gluon plasma at a pseudo-critical temperature $T_c \simeq 155MeV$ [2],[3] which is accompanied by the chiral symmetry restoration. The reduction of the chiral condensate expectation value predicted by the calculations is shown in Fig.1.

Experimentally, the structure of the QCD phase diagram is studied by means of heavy ion collisions over a broad energy range. Temperature and baryochemical potential are extracted from fits to hadronic yields measured by various detectors at LHC, RHIC, SPS and SIS18 at the lowest energy frontier. The extracted T, μ_b values obtained by the statistical hadronization model of [4] are presented in Fig.1. Since these temperatures characterize the late stage of the collision, where hadrons decouple from the strongly interaction system (so called freeze-out), it is expected that at highest energies initial temperatures are higher than the T_c and quark-gluon plasma is created. In the course of the collision evolution, QGP matter rapidly expands and when temperature drops to T_c, it hadronizes to a hadron gas. Dashed lines, shown in Fig. 1, depict hypothetical trajectories of collision at SPS energy of 158 AGeV and at 1.23 AGeV at SIS18.

At energies of around $1 - 2$ GeV per nucleon, where HADES experiment is operating, nuclear matter can be compressed to two-three times the ground state density and collective kinetic energy is dissipated into intrinsic degrees of freedom. As a result, some nucleons (about $20 - 30\%$) are excited to baryonic resonances and in the final state of the reaction mesonic states (mainly pions) are observed with increasing abundances as the center-of-mass energy of the collision rises. The system is characterized by a large baryo-chemical potential (baryon dominated matter in contrast to the meson dominated matter produced at higher energies) and moderate temperatures of about $50 - 70$ MeV. It resembles the matter created in neutron star mergers where similar temperatures can be reached [5]. Compressing nuclear matter can lead to a significant overlap of baryons which at some densities start to share their pion cloud content, hence creation of a new form of matter may be expected.

A scientific challenge, both to theory and experiment, is to understand the microscopic properties of such exotic matter over a broad range of the temperature and the baryo-chemical potential spanned by various experiments.

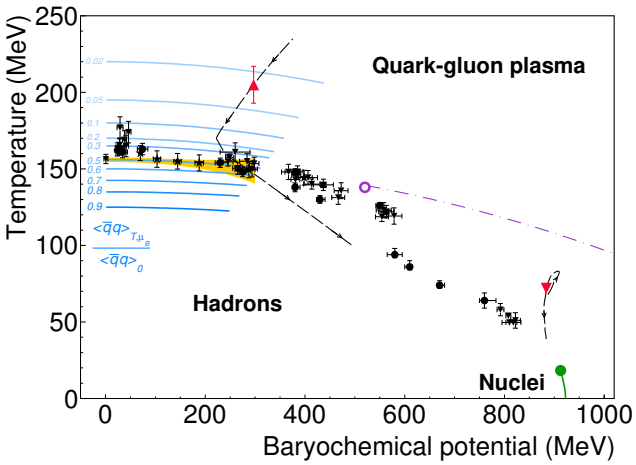

Figure 1. QCD phase diagramme. Experimental black points were obtained from a fit using statistical hadronization model to the hadron yields measured in various Heavy ion experiments [4]. The expectation values of the chiral condensate relative to the vacuum as constrained by the lattice calculations [2] are depicted as blue curves. The yellow band is the crossover region. The dotted–dashed purple curve shows the conjectured first-order phase transition, which terminates in a second-order QCD critical point (open purple circle), whose exact location is a matter of debate. The red upright triangle displays the temperature deduced from the dielepton measurements (see text for details). Lines with arrows show hypothetical trajectories for HI collisions at SPS and SIS18. Figure taken from [5]

.

One of the most promising probes used to examine properties of such exotic state of matter are dileptons. They are highly penetrating probes, not suffering strong final state interactions, hence providing insight into all phases of the collision. The dilepton radiation can be understood as emission of virtual photons in analogy to photon radiation from hot medium with the additional important parameter namely the mass. The spectral distribution of dileptons is strongly influenced by the temperature of collisions and the microscopic properties of medium. This connection can be understood by inspection of a formal expression for the differential thermal dielectron rate from a four volume of a medium characterized by T, μ_b : [6]

$$\frac{dR}{d^4qd^4x} = -\frac{\alpha^2}{\pi^3}\frac{L(M^2)}{M^2} Im\Pi_{em}(M, p, T, \mu_b) f^B(q_0, T) \quad (1)$$

In the formula $Im\Pi_{em}$ is the imaginary part the quark current-current correlator depending on the dilepton mass $M = q^2$ and the momentum p, $f^B(q_0, T)$ is the thermal Bose distribution function and $L(M^2) = (1+\frac{2m_l^2}{M^2})\sqrt{1-\frac{4m_l^2}{M^2}}$ is the lepton phase space element (it approaches one above

dilepton threshold $M > 2m_{l+l^-}$). $Im\Pi^{had}_{em}(M)$ is very well known in vacuum from e^+e^- annihilation into hadrons. It is flat in the Intermediate Mass Region (IMR): $3 > q^2 > 1.5$ GeV/c^2, as predicted for $e^+e^- \rightarrow q\bar{q}$ transition by perturbative QCD, and is dominated by $\rho/\omega/\phi$ resonances below (Low Mas region-LMR). The latter one demonstrates Vector Meson Dominance in the photon-hadron transitions, a phenomenon playing a prominent role in low energy hadron physics. In particular, the short lived ρ meson ($c\tau$ = 1.3 fm/c) with strong coupling to pions plays the most important role in the radiation from the fireball created in heavy ion collisions.

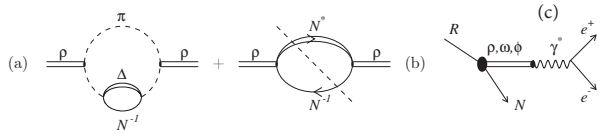

Figure 2. Schematic presentation of main graphs entering in-medium calculation of the ρ meson spectral function (a,b) and the relation to the elementary process of Dalitz decay of baryon resonance (c).

Various model calculations of the $Im\Pi_{em}$ for the non-vanishing T, μ_b predict its significant modifications in LMR due strongly modified ρ meson spectral function (for overview see [7]). The respective interactions can be grouped in two types of graphs (see Fig. 2) including pion-loop modifications (a) and baryon-ρ meson interactions (b). Systematic comparisons of the model calculations to the experimental data collected at SPS and RHIC reveals the dominant role of the baryon induced interactions [8],[9]. The modifications of ρ meson spectral function can be linked, though not directly, with chiral symmetry restoration by means of QCD and Weinberg sum rules. Indeed, the hadronic models do not include explicitly quantities characterizing QCD vacuum properties like quark or gluon condensates but the connection between the splitting of spectral functions of the chiral partners $\rho - a_1$ and the quark condensate and the pion decay constant is provided, as for example by the Weinberg sum rules [10].

$$\int ds \frac{1}{s}(D^V_\rho - D^a_{a1}) = f_\pi^2; \qquad (2)$$

$$\int ds(D^V_\rho - D^a_{a1}) = {f_\pi}^2 m_\pi^2 = -2m_q < q\bar{q} > \qquad (3)$$

Using the results of the hadronic models for the ρ meson in-medium spectral function and lattice results on the quark condensate evolution as a function of the temperature merging of the two spectral function has been demonstrated at $T = T_c$ and vanishing μ_b [11]. This signals the behaviour expected for the chiral symmetry restoration.

Another important benefit from dilepton measurements in heavy ion collisions is the ability to extract the temperature of the collision. Indeed, although the equation 1 holds for the radiation rate at the defined T, μ_b it has been demonstrated by comparison of various model calculations with the dilepton data that the time evolution of the fireball can be successfully implemented in the dilepton calculations (see [9],[12]). The two red triangles shown in Fig. 1 are the averaged temperatures of early collision phases extracted by analysis of the thermal radiation in IMR by the NA60 experiment at CERN and in the LMR by the HADES experiment at GSI, described in more details below. Note, that in both cases, the extracted temperatures are slightly higher than the one obtained from the analysis of the hadron spectra (black points).

Results of the hadronic models, however, strongly rely on the experimental input characterizing the vector meson-baryon couplings. The respective constraints on the calculations are provided by poorly known baryon resonance-vector meson branching ratios and constrains from photo-absorption data. The latter strongly rely on extrapolation from the photon point to the meson poles based on the Vector Meson Dominance. Both aspects, can be scrutinized more directly by measurements of baryon resonance radiative decays involving virtual timelike photons ($q^2 > 0$), described in more details in next section. This elementary process, shown in Fig.2 by the graph (c), is directly connected to the graph (b) by the respective cut. These decays are being investigated, for the first time, by HADES by studies of exclusive dielectron channels in proton and pion induced reactions, as described in this contribution.

2 Baryon transition form-factors

The matrix element for a radiative transition of an excited baryon to its ground state $\mathcal{M}(R \rightarrow N\gamma^*)$ by means of massive timelike photon can be expressed as a coherent sum of helicity amplitudes $A_{3/2}(q^2)$, $A_{1/2}(q^2)$ and $S_{1/2}(q^2)$, defined in the resonance decay frame [13]. The first two amplitudes are related to the transverse photon polarization while the last one is related to the longitudinal photon polarization. In the limit of $q^2 = 0$ (real photon) $S_{1/2}$ vanishes. The helicity amplitudes have been determined in space like region ($q^2 < 0$) for several resonances in electro- and photo- production experiment (for review see [14]). They are, however, unknown in the timelike region which is accessible by the Dalitz decays $R \rightarrow N\gamma^*$.

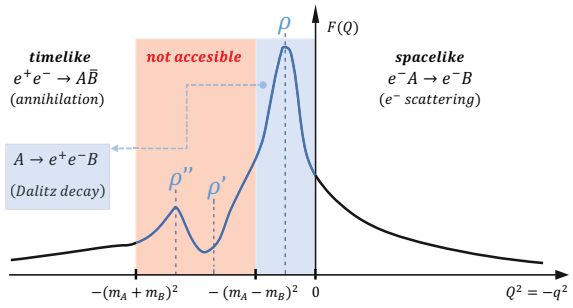

Figure 3. A schematic view of etFF evolution as a function of q^2 and kinematic conditions relevant for experiments in timelike and spacelike regions.

The respective differential decay width for the Dalitz decay $d\Gamma(R \rightarrow Ne^+e^-)/dM_{l^+l^-}$ depends on the resonance

mass, spin and parity and is expressed as a function of the magnetic ($G_M(q^2)$), the electric ($G_E(q^2)$) and the Coulomb ($G_C(q^2)$) transition Form Factors (etFF). For the $J \geq 3/2$ (for example $\Delta(1232)$) there are three etFF and for $J < 3/2$ only two (for details see[13]). The relations between the helicity amplitudes and the etFF are given by linear transformations [13]. The calculations predict a strong dependence of the form-factors on the dielectron mass reflecting the important role of the intermediary vector meson fields in the transition, as predicted by VMD (see graph (c) in Fig. 2. Particularly the role of the broad ρ meson is visible in the strong enhancement of the transition rates for the dilepton masses even below the meson pole. Various implementations of VMD provide, however, different results, which calls for experimental constraints.

Fig. 3 displays a schematic view of the evolution of etFF as a function of q^2 and kinematic limits for measurements in spacelike and timelike regions

3 HADES experiment

HADES (High Acceptance DiElectron Spectrometer) is an apparatus installed at synchrotron SIS18 at GSI/FAIR in Darmstadt [15]. It has a large acceptance for charged particles and is optimized to identify very rare electrons and positrons in a hadron rich environment, which exceeds the electron signal by many orders of magnitude in multiplicity.

The HADES spectrometer consists of six identical sectors covering the full azimuth and polar angles from 18° to 85° measured relative to the beam direction. Each sector of the spectrometer contains a Ring-Imaging Cherenkov Detector (RICH) operating in a magnetic field-free region, two drift chambers (MDCs) in front of a toroidal magnetic field, and two outer MDCs behind the magnetic field, time-of-flight detectors, based for $\theta > 45°$ on scintillator rods (ToF) and for $\theta < 45°$ on resistive plates (RPC), combined with an electromagnetic calorimeter (ECAL) that replaces the Pre-shower detector used in previous campaigns. At forward angles ($\theta < 8°$) the detection of charged particles will be extended in 2019 by two straw tube tracking stations, developed for the PANDA detector, and a RPC ToF wall. This ensemble constitutes the Forward Detector.

Momentum measurement of charged particles in HADES is achieved by tracking the particles in front of and behind the toroidal field generated by six superconducting coils arranged symmetrically around the beam axis. A powerful and flexible trigger system selects events with defined multiplicity or topological pattern of charged hits in the TOF detectors. A major improvement of the spectrometer in terms of granularity and particle identification capability was achieved with the RPC time-of-flight detectors. The Forward Detector will significantly increase the acceptance for hyperon reconstruction in proton induced reactions.

The HADES detector operates with primary proton and Heavy Ion (HI) beams obtained from SIS18 and secondary pion beams. Runs were performed with proton (E_{kin} = 1.25, 2.2, 3.5 GeV), deuteron (E_{kin} = 1.25 GeV) beams on LH−2 target and with proton beam on Nb (E_{kin} = 3.5 GeV) target. The primary goal of these experiments was to provide a reference for HI reactions, particularly for Dalitz decays of baryon resonances and non-resonant nucleon-nucleon bremsstrahlung which had not been previously measured. Some highlights from these measurements are given in the next subsections.

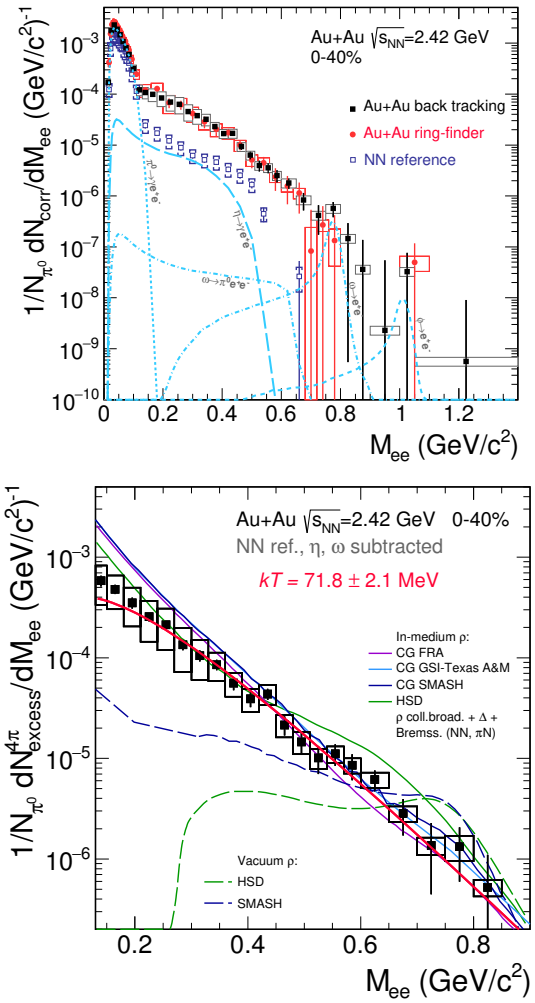

Figure 4. Top: Dielectron invariant mass distribution measured in Au+Au collisions compared to the freeze-out contribution from mesonic sources and the radiation from first chance baryonic contributions ($N-N$ -reference)(see text for details). Bottom: Dielectron excess yield extracted by subtracting the meson contributions as well as the $N-N$ reference normalized to the number of neutral pions. Red curve:thermal fit, dashed curves: ρ-meson vacuum line shape from HSD [18] and from SMASH [19] transport model calculations normalized to the respective number of neutral pions. Solid green curve: incoherent sum of all contributions: $\Delta \rightarrow Ne^+e^-$, $N-N$ and $\pi-N$ bremsstrahlung and in-medium ρ (collisional broadening scenario) from HSD . The dark-blue [19], blue[20] and pink [12] are curves show the results of three versions of coarse-grained calculations using in ρ medium-spectral functions from microscopic calculations [7].

3.1 Radiation from A+A collisions

Heavy ion experiments were conducted with $C+C$ (E_{kin} = 1.0, 2.0 AGeV), $Ar+KCl$ (E_{kin} = 1.76 AGeV) and $Au+Au$

E_{kin} = 1.25 AGeV collision systems. The results from the $C+C$ experiments demonstrated that the dilepton production in the light system can be successfully described by a superposition of nucleon-nucleon collisions, measured in separate runs, without any need to include in-medium effects [16].

However, in the medium heavy $Ar+KCl$ [17] and truly heavy $Au+Au$ system [5] a systematic excess of the radiation over the contributions expected from decays of neutral mesons (π, η) produced at freeze-out and from baryonic sources (Δ Dalitz decays and $N-N$ bremsstrahlung) determined from $N-N$ reactions (see next section). The latter is obtained as an average of the radiation measured in $p+p$ and $p+n$ collisions scaled by the respective number of pions. The scaling accounts for differences in the number of participating nucleons in the collision systems. The excess is clearly visible in comparison of the measured mass distribution to the aforementioned sources shown in top of Fig. 4

The excess radiation is shown in the lower part of Fig.4 as a function of the invariant mass in comparison to various model calculations (for references see [5]). The predictions of various models using thermal ansatz and applying Eq. 1 with the ρ meson spectral function obtained from the hadronic models are indicated as CG in Fig.4. The results explain the measured yield well and confirm a strong coupling of baryon resonances to the ρ meson and consequently its almost complete melting in dense baryonic medium (compare to the ρ vacuum spectral function shown by dashed lines). This conclusion justifies also a thermal fit (with function $dN/dM \simeq M_{ee}^{3/2} exp(-M_{ee}/kT)$ which provides the averaged temperature ($kT = 71.8 \pm 2.1$ MeV) of the radiating matter. The results of transport calculations (HSD) which use empirical scaling of the ρ meson width with the density also describe data reasonable well (except some overestimation at the meson pole). This calculation do include, however, explicit contributions from multistep processes in the dense phase of the collisions involving radiation from Δ and $N-N$ bremsstrahlung. These contributions are included in the hadronic model calculations in the spectral function. In particular these sources contribute below the two pion mass cut-off visible in the vacuum spectral function assumed in the HSD calculations (green-dashed line).

These HADES results constitutes an important reference for the planned beam energy scan within Compressed Baryonic Matter programme at FAIR and the lowest energy point in the measurement of dilepton excitation function.

3.2 Radiation from N-N collsions

The measurement with proton beams with E_{kin} = 1.25 GeV provides clean basis for studies of baryonic sources of dielectron pairs relevant for heavy ion reactions studied by HADES. The most important are the Dalitz decays of baryonic resonances $N^*(\Delta^*) \rightarrow Ne^+e^-$ and nucleon-nucleon bremsstrahlung. The meson contribution is limited to the π^0 Dalitz decay contributing to the dielectron spectrum with invariant masses smaller than the pion mass. The exclusive final states ppe^+e^- and pne^+e^-, separated in the $p+p$ and quasi-free $p+n$ collisions (from $p+d$) at the same energy allowed also for the direct comparison of the two collisions systems.

In $p+p$ collisions the dilepton pairs with invariant masses $M_{e^+e^-} > 0.15$ GeV/c^2 are consistently explained by the $\Delta^* \rightarrow Ne^+e^-$ decay, with only small $p-p$ bremsstrahlung contribution (see Fig. 5). This has been concluded from the combined analysis of the one pion ($pp\pi^0$, $pn\pi^+$) and the dielectron (ppe^+e^-, $ppe^+e^-\gamma$) exclusive final states [21],[22]. The latter allowed to access both $\Delta \rightarrow p\pi^0(e^+e^-\gamma)$ and $\Delta^+ \rightarrow pe^+e^-$ Dalitz decay channels. The Δ Dalitz decay was identified for the first time with the branching ratio $BR = (4.19 \pm 0.62 syst. \pm 0.34 stat.) \times 10^{-5}$. The Δ isobar production cross section was determined from the energy dependent Bn-Ga PWA analysis performed on the HADES one pion channels and 13 data sets measured at PNPI at lower energies [22]. The PWA analysis shows that at the energy of $\sqrt{s} = 2.42$ GeV the dominant contribution is given by the production of $\Delta(1232)$ in the intermediary state ($\simeq 70\%$ of the total cross section in the $pp\pi^0$ final state). The remaining part originates from the Roper excitation with a small non-resonant contribution.

Fig. 5 shows comparisons of the $p\pi^0$ invariant mass distribution reconstructed from the hadronic final state (open squares) and the dielectron $\Delta \rightarrow p\pi^0(e^+e^-\gamma)$ (black dots) to the PWA solutions (blue histogram). One can see a very good agreement between the data from the two reaction channels and also to the PWA solutions both in shape and in absolute scale (note that dielectron channel was not included in the PWA analysis). Similar conclusion was drawn from all studied differential distributions (invariant mass, angular distributions in the helicity and Gottfried-Jackson frames), for details see [21].

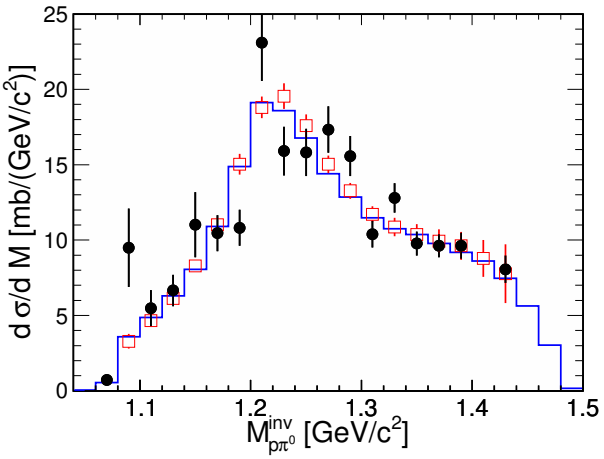

Figure 5. Dielectron data points after acceptance and branching ratio for $\pi^0 \rightarrow e^+e^-\gamma$ decay corrections (black dots) compared with the data from the exclusive $pp\pi^0$ channel (red open squares). The histogram shows total PWA solution (solid blue) obtained for the hadronic channel

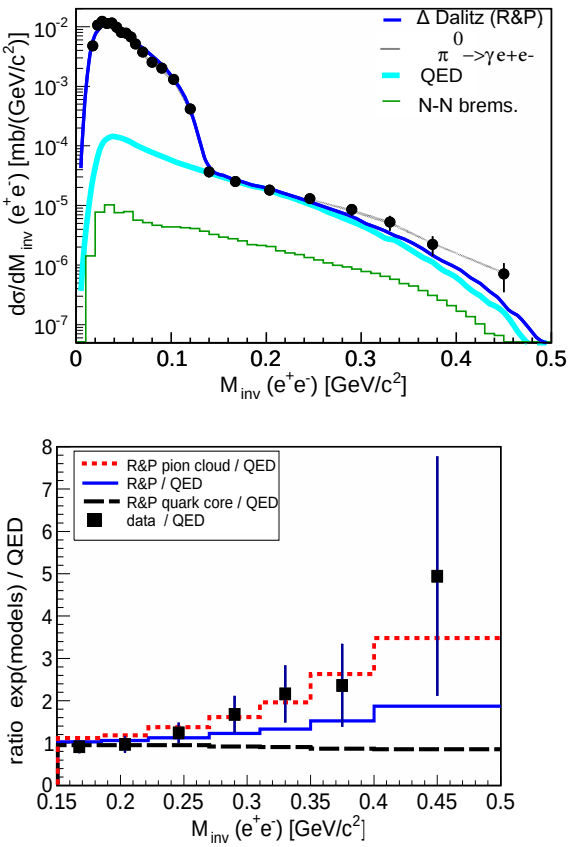

Figure 6. Upper: Dielectron invariant mass distribution from $p+p$ collisions at E_{kin} = 1.25 GeV compared to calculations using the Δ (model of Ramahlo and Pena (R&P)-blue [23] and for the point-like Δ (QED-cyan), π^0 Dalitz and $p+p$ bremsstrahlung. Bottom: Ratio of the measured dielectron invariant mass from the $\Delta(1232) \rightarrow pe^+e^-$ decay to the model of point-like particle (QED) compared to the Ramahlo and Pena (R&P) full model (blue) and assuming dominance of the photon-quark core (black dashed) and photon-pion-cloud contributions (red dashed) (see text and [21] for details).

From the measured differential mass distribution a ratio of the data to the calculations of Δ(1232) Dalitz decay assuming constant etFF $|G_M| = 3$ (value at the photon point) $G_E = G_C = 0$, labelled in Fig. 5 as QED, have been calculated. A slight increase of the effective etFF as a function of the photon virtuality ($q^2 = M_{e+e-}$) can be clearly seen in Fig.6. This is in agreement with the covariant quark model of [23] assuming significant contribution from the virtual photon-pion cloud coupling. In the model this coupling to the ρ meson is much stronger than to the quark core (compare dashed black and red dashed) and produces the aforementioned enhancement. Furthermore, since the $N-\Delta$ transition in the spacelike region is dominated by the spin-flip magnetic transition it can be expected that the dominant role in the measured low q^2 region is played by $G_M(q^2)$ and consequently that the virtual photons are preferentially transversally polarized.

This conclusion is corroborated by the analysis of the angular distributions of either of both leptons in the rest frame of the virtual photon (helicity frame). According to calculations [24], it should obey $\simeq 1 + Bcos^2\theta$ distribution, with B=1 for the transversely polarized photons. The anisotropy coefficient deduced from the data analysis $B = 1.17 \pm 0.34$ confirms the expectation.

However, the $n+p$ data exhibits a very different shape above π^0 mass as compared to the $p+p$ measured at the same energy (see Fig. 7) [25]. This can be clearly recognized as an apparent excess above the Δ contribution (red dashed line), which has a similar shape for the two reactions but explains the $p+p$ data very well. This finding was not completely unexpected since various calculations of N-N bremsstrahlung, defined here as the non-resonance contribution that has to be added coherently to the Δ excitation, performed already in the $90's$ in the framework of One Boson Exchange (OBE) models [26],[27], [28] predicted a stronger contribution of this non-resonance dielectron production in the neutron-proton interactions. However, the calculations showed a strong sensitivity of the dielectron yield on the off-shell electromagnetic form factors of nucleons, and on the etFF of Δ(1232). Also modelling of nucleon-nucleon interaction requires form-factors to dress the respective vertices and various nucleon-meson coupling constants which needs to be fixed from experimental data. While the latter could be fixed to some extent from the data on meson production close to the threshold, the first ones can only be inferred from the dilepton data. It is therefore not surprising that the model predictions could not explained both dielectron exclusive channels $p+p$ and $n+p$ because the relevant precision data were missing. This has changed with the new HADES data and the most recent calculations performed by [29] in OBE which account almost completely for the missing yield (dashed-dotted blue line in Fig. 7) and explain also $p+p$ data. In this calculations it was found that an important role is played by graphs accounting for the radiation from charged pion exchange line. It has been also emphasized that the electromagnetic pion form factor, dominated by the ρ meson, plays an essential role in the successful description of data. This is another example of sensitivity of dielectron radiation to the etFF's of hadrons in timelike region.

The alternative model of [30] assuming $\Delta\Delta \rightarrow \rho np \rightarrow npe^+e^-$ has been put forward for the explanation of $n+p$ data. It is shown by the solid green line in Fig.7. The salient feature of both calculations is the transition from the Δ Dalitz dominated region $0.14 < M_{e^+e^-} < 0.28$ GeV/c^2 to the higher mass region which is dominated by the off-shell ρ contribution.

Although both models do not provide more differential information, this behaviour seems to be corroborated by the electron angular distributions in the helicity frame. Whereas, see Fig. 8, in the lower mass region the distribution reveals the characteristic $1 + Bcos^2(\theta_l)$ shape with $B \simeq 1$, measured also for the Δ in the $p+p$, at larger invariant masses the distribution changes character and the anisotropy parameter takes the value $B = 0.25 \pm 0.35$. This can be interpreted as dominance of the emission from the meson line through the off-shell ρ meson. Indeed, the anisotropy parameters B extracted in the reference frame

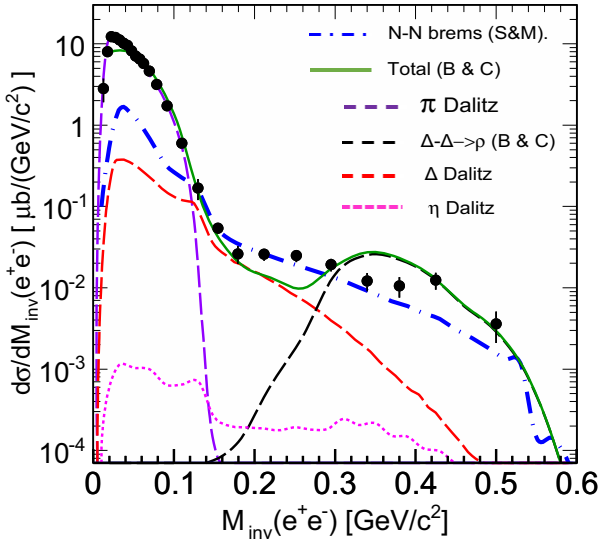

Figure 7. Invariant mass distribution of dielectrons measured in a quasi-free $n + p$ collisions at $E_{kin} = 1.25$ GeV compared to the $N - N$ bremsstrahlung model of [29] (blue-dashed) and the model of [30] (green) decomposed in the Δ Dalitz (red dashed), ΔΔ fusion and π^0 Dalitz (dashed-violet) contributions.

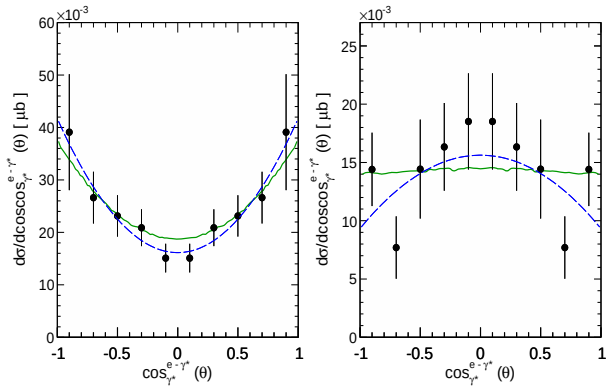

Figure 8. Angular distributions (black dots) of the leptons in the rest frame of the virtual photon for the dielectron mass of $0.14 < M_{e^+e^-} < 0.28$ GeV/c^2 (left panel), and with respect to the direction of the charged pion exchange for dielectrons with $M_{e^+e^-} > 0.28$ GeV/c^2 (right panel) corrected for the detector acceptance. The solid green curves display predictions from the simulations where the dominant source is the Δ(1232) in the low mass bin and the ρ in the high-mass bin (assumed to be isotropic). The dashed blue curve shows a fit with a function $A(1 + Bcos^2(\theta_e))$

with z axis fixed along the direction of the exchanged charged pion becomes slightly negative $B = -0.4 \pm 0.25$. This can can be compared to the value $B = -1$ expected for the pion annihilation [24].

Measurements of dielectron production in proton-proton collisions with $E_{kin} = 3.5$ GeV reveal importance of higher mass resonances [31, 32]. From the one pion exclusive channels $pp\pi^0$ and $pn\pi^+$, measured in the same experiment, cross sections for Δ and N^* resonances have been estimated by means of a resonance model assuming two step reaction mechanism with the intermediate resonance formation. The resonance model applied in the HADES analysis was inspired by the calculations presented in [33] applied in transport models for particle production at SIS18 energies. In the HADES model empirical angular distributions for the production of resonances showing a strong forward-backward peaking which is characteristic for peripheral reactions have been added in accordance to the measured distributions. A good description of the experimental data in the detector acceptance has been achieved allowing for an extrapolation to the full solid angle and an extraction of the pion production cross sections which are compatible with the word data (for details see [32]). Recently, the HADES resonance model has been successfully extended to two pion production (see contribution of A. Belounnas to this conference).

In the exclusive ppe^+e^- channel dielectron production from the baryon resonance Dalitz-decays and two-body $\rho/\omega \to e^+e^-$ meson decays have been concluded as dominant sources of the pair production. In particular, a significant yield below the vector meson pole has been identified and attributed to the Dalitz decays of Δ, N^* resonances proceeding through the intermediate ρ meson state, as explained in more details below.

Indeed, using estimates of production cross sections following form the pion analysis contributions to the dielectron spectrum was calculated. The dielectron yields, presented with dashed blue line in the upper panel of Fig.9, were obtained using constant eTFF, as predicted in [13] [34]. The uncertainty in the production cross sections of baryon resonances is presented by the grey band spanned around the dashed line. As one can see, the total contribution from the higher mass resonances (green line) is larger than from the Δ(1232), shown by the red line, and confirms importance of higher mass resonances. The model, however, cannot reproduce the measured yield and suggests strong off-shell vector meson couplings. These couplings modify the decay vertex of the resonance by means of the respective etFF (see graph (c) in Fig. 2). Since the mass dependence of the respective eTFF are not known, an alternative approach for the Dalitz decay of resonances was applied. It assumes a factorization of the $R \to pe^+e^-$ process into two steps $R \to \rho N$ and $\rho \to e^+e^-$ which could be calculated using the resonance branching ratios to the ρN from PDG (from 2014). Similar approach is also implemented in transport codes (GiBUU, UrQMD or recently SMASH) to account for the off-shell ρ meson contributions. Note that on-shell ρ meson contribution known from the two-pion production is included in the cocktail (violet line) but can not explain the apparent excess in the data, too. The GiBUU calculations utilizing the factorization scheme, shown in the lower panel by black line, come closer to the data and explain also the invariant mass distributions of the combined system pe^+e^-. A slightly better description is achieved using the same prescription but the cross section for resonance production extracted from the HADES resonance model (dotted line). The main dif-

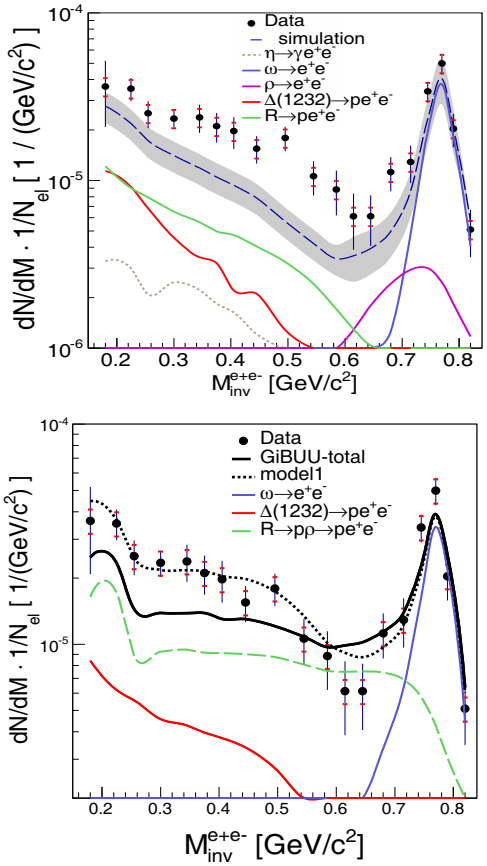

Figure 9. Top: Invariant mass distribution of dielectron pairs measured in the exclusive channel $p + p \rightarrow ppe^+e^-$ at E_{kin} = 3.5 GeV compared to cocktail of baryonic and mesonic sources. The contribution from baryon resonances is separated into contributions from Δ(1232) (red line) and higher mass states (green) assuming constant etFF. Bottom: same data compared to calculations using for the baryon resonance two step decay involving coupling to intermediate ρ meson state (for details see text).

ference in the HADES resonance model is a higher cross section for the $N^*(1520)$ (factor 8), slightly lower (factor 2) cross sections of the other resonances (for details see [32]) and lower branching ratio for the resonance decays (for details see [32]). The latter one was taken from the Bonn-Gatchina upper estimates of the $R \rightarrow N\rho$ instead of the respective branching ratios given in PDG (2014). One should note, that in the recent PDG those values have been removed and await new experimental input. The contribution of higher mass resonances (dashed green curve) is given by the decays of $N^*(1520)(38\%)$, $N^*(1720)(22\%)$, $\Delta(1620)(15\%)$ and $\Delta(1905)(6.5\%)$.

3.3 Pion beams in HADES

Recently, successful measurements were completed with HADES using secondary pion beams [35]. The pion beam was obtained from a primary ^{14}N beam with an intensity of 0.8-1.0×10^{11} ions/spill impinging on a beryllium (^{9}Be) target (see Fig.11). Beam intensity for negative pions as a function of the momentum scaled to the space charge limit of SIS18 are displayed in Fig. 10 [36].

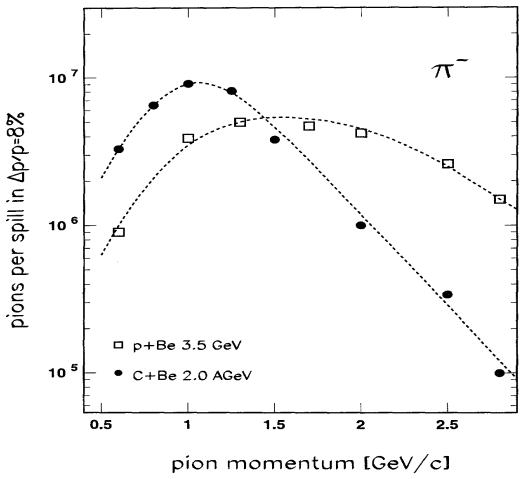

Figure 10. Negative pion yields at the HADES target point as a function of the momentum scaled to the space charge limit of SIS18.

Produced pions were transported by the beam line consisting of 9 quadrupole and 2 dipole magnets to the HADES target located 33 meters downstream from the production point (see Fig. 11). The maximum pion intensity of 10^6 pions/spill was achieved at a momentum p = 1.0 GeV/c. The intensity decreased by a factor 2 for the pion momentum range p = 0.65 − 0.8 GeV/c investigated in the measurement. Four reference beam momenta p = 656, 690, 748, 800 MeV/c were selected using different settings of currents in the magnets of the beam line. The differential transmission distribution of the pions as a function of the momentum can be approximated by Gaussian with a typical width of ≃ 1.7%. Further improvement to reduce the pion beam momentum resolution to δp = 0.3% was provided by a dedicated in-beam tracking system CERBEROS positioned in the beam line as shown in Fig.11. The detectors provide (x, y) coordinates of pion hits, with precision given by the 780μm pitch of strips. The hit coordinates were used to determine the optical properties of the beam line, which are needed for an event-by event momentum reconstruction, as described in details in [35]. The in-beam detector system included also a segmented START detector, made from mono-crystalline diamond material, placed in front of the HADES target.

Resonance formation in s-channel with a fixed mass presents an important advantage of pion induced reactions w.r.t reactions with proton beams where contributions from many resonances with different masses must be considered. The measurement was focused on two pion and dielectron production in the second resonance region with the main goal to characterize the role of off-shell ρ meson couplings to the $N^*(1520)$ and $N^*(1535)$ resonances [37]. A combination of two-pion with dielectron decay channels, that can be measured only by HADES, offers an unique possibility to explore baryon resonance decay channels into ρ and dielectron channels. To isolate the

ρ meson decay channels a combined Partial Wave Analysis of the hadronic channels in pion and photon induced reactions has been performed within Bonn- Gatchina approach. The excitation function of the different partial waves and $\Delta\pi$, $N\sigma$ and $N\rho$ isobar configurations has been determined. The N(1520) resonance is found to dominate the $N\rho$ final state with the branching ratio BR = 12.2 ± 1.9% [37].

Preliminary results are presented in reports of B. Ramstein and I.Ciepal to this conference.

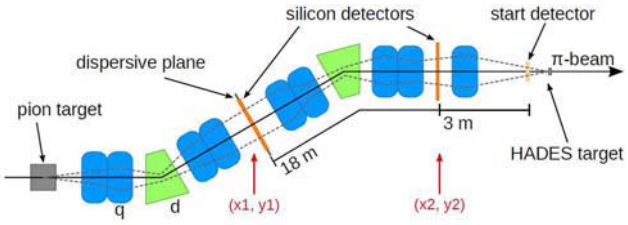

Figure 11. Pion beam line from the production point (pion target) to the HADES target position. Quadrupole and dipole magnets guide the pions (the dashed line) through the in-beam tracking detectors (indicated by the arrows).

4 Summary and outlook

Our recent studies of the baryon resonances in the exclusive channel $NN \rightarrow NNe^+e^-$ revealed patterns of far off-shell ρ production followed by dielectron decay. This raises the question to what extent the baryon meson cloud is instrumental in transferring excitation energy into the vector meson and to virtual photon with the invariant mass $m_{e^+e^-}$. This process is characterized by the interaction vertex described by the electromagnetic transition form-factors of the resonances in the (soft) timelike region where $0 < q^2 = (m_{e^+e^-})^2 < (M_R - M_N)^2$ with M_R and M_N the resonance and the nucleon mass, respectively. With the secondary pion beams [35] at GSI/FAIR and the HADES detector, one has an unique opportunity to explore radiative and Dalitz decays of baryon resonances into much more details. The first experiment, studying two pion and dielectron production in the second resonance region, confirms strong coupling for $N^*(1520)$ to the off-shell ρ meson in both two-pion and dielectron channel. The research programme formulated by HADES wihin FAIR Phase0 anticipates an energy scan in the third and fourth resonance region with high statistic measurements of neutral and charged mesons and dielectrons. This program is also extended to measurements of radiative decays of baryons containing strangeness [38]. In a similar way, as for the non-strange baryons Dalitz decays of excited hyperon states, Λ^*, Σ^* in pion and proton induced reactions at maximum SIS18 energies has been proposed. Especially, transitions of narrow $\Lambda(1520)$ and $\Sigma(1385)$ states to Λ and dielectron pair seems to be ideal candidates for such measurements. Also high statistics measurements of hadronic decays of $\Lambda(1405)$ and double strange cascades are considered. In particular, measurements of the controversial $\Lambda(1405)$ in pion-induced reactions, will provide important complementary information to the one already obtained by HADES in $p + p$ collisions to constrain the model calculations and to unravel the nature of $\Lambda(1405)$.

HADES results from heavy ion reactions demonstrate also the particular role played by vector meson-baryon interactions in the understanding of the dielectron radiation from dense baryonic matter. A better understanding of the coupling of baryonic resonances to intermediary ρ mesons is mandatory to validate emissivity calculations for hadron-resonance matter. Such studies can therefore pave the way for searching new states of matter with the upcoming Compressed Baryonic Matter program at FAIR's SIS100.

Acknowledgments

SIP JUC Cracow, Cracow (Poland), National Science Center, grants: 2016/23/P/ST2/04066 POLONEZ funded from the European Union's Horizon 2020 research and innovation programme under the Marie Sklodowska-Curie grant agreement No 665778, 2017/25/N/ST2/00580, 2017/26/M/ST2/00600; TU Darmstadt, Darmstadt (Germany), VH-NG-823, DFG GRK 2128, DFG CRC-TR 211, BMBF:05P18RDFC1; Goethe-University, Frankfurt (Germany) and TU Darmstadt, Darmstadt (Germany), ExtreMe Matter Institute EMMI at GSI Darmstadt; TU München, Garching (Germany), MLL München, DFG EClust 153, GSI TMLRG1316F, BmBF 05P15WOFCA, SFB 1258, DFG FAB898/2-2; NRNU MEPhI Moscow, Moscow (Russia), in framework of Russian Academic Excellence Project 02.a03.21.0005, Ministry of Science and Education of the Russian Federation 3.3380.2017/4.6; JLU Giessen, Giessen (Germany), BMBF:05P12RGGHM; IPN Orsay, Orsay Cedex (France), CNRS/IN2P3; NPI CAS, Rez, Rez (Czech Republic), MSMT LM2015049, OP VVV CZ.02.1.01/0.0/0.0/16 013/0001677, LTT17003.

References

[1] C.D Roberts, Few Body, Syst. **58**,5(2017) , see also contribution to this conference
[2] Borsanyi, S. et al., J.High Energy Phys. **73**, 2010:73 (2010)
[3] Bazavov, A. et al.,Phys.Lett.B **795**,15(2019)
[4] Andronic, A. et al., Nature **561**, 321 (2018).
[5] Adamczewski-Musch, J. at al. , Nature Physics (2019) doi.org/10.1038/s41567-019-0583-8
[6] L. McLerran and R. D. Pisarski, Nucl. Phys. A **796**, 83 (2007)
[7] R. Rapp and J. Wambach, Adv. Nucl. Phys. **25**, 1 (2000)
[8] H. van Hees and R. Rapp, Nucl. Phys. A **806** (2008) 339
[9] R. Rapp and H. van Hees, Phys. Lett. B **753** (2016) 586
[10] S. Weinberg Phys. Rev. Lett **18**, 507 (1967)
[11] P. M. Hohler and R. Rapp, Phys. Lett. B **731** (2014) 103

[12] S. Endres, H. van Hees and M. Bleicher, Phys. Rev. C **92**, 014911 (2015), Phys. Rev. C **93** (2016) no.5, 054901,

[13] M. I. Krivoruchenko, B. V. Martemyanov, A. Faessler and C. Fuchs, Annals Phys. **296**, 299 (2002)

[14] I. G. Aznauryan and V. D. Burkert, Prog. Part. Nucl. Phys. **67**, 1 (2012)

[15] G. Agakishiev *et al.* [HADES Collaboration], Eur. Phys. J. A **41** (2009) 243 doi:10.1140/epja/i2009-10807-5 [arXiv:0902.3478 [nucl-ex]].

[16] G. Agakishiev *et al.* [HADES Collaboration], Phys. Lett. B **690**, 118 (2010)

[17] G. Agakishiev *et al.* [HADES Collaboration], Phys. Rev. C **84** (2011) 014902 doi:10.1103/PhysRevC.84.014902 [arXiv:1103.0876 [nucl-ex]].

[18] Bratkovskaya, E. L. et al., Phys. Rev. C **87**, 064907 (2013)

[19] Staudenmaier, J., et al. Phys. Rev. C **98**, 054908 (2018)

[20] Galatyuk, T., Eur. Phys. J. **52**A, 131 (2016)

[21] J. Adamczewski-Musch *et al.* [HADES Collaboration], Phys. Rev. C **95** (2017) no.6, 065205

[22] G. Agakishiev et al. (HADES Collaboration), Eur. Phys. J. A **51**, 137 (2015).

[23] G. Ramalho and M. T. Pena, Phys. Rev. D **85**, 113014 (2012)

[24] E. L. Bratkovskaya, O. V. Teryaev, and V. D. Toneev, Phys. Lett. B **348**, 283 (1995)

[25] J. Adamczewski-Musch *et al.* [HADES Collaboration], Eur. Phys. J. A **53**, no. 7, 149 (2017) doi:10.1140/epja/i2017-12341-3 [arXiv:1703.08575 [nucl-ex]].

[26] M. Schafer, H. C. Donges, A. Engel and U. Mosel, Nucl. Phys. A **575**, 429 (1994)

[27] M. Schafer, H. C. Donges and U. Mosel, Phys. Lett. B **342**, 13 (1995)

[28] F. de Jong and U. Mosel, Phys. Lett. B **392**, 273 (1997)

[29] R. Shyam and U. Mosel, Phys. Rev. C **79**, 035203 (2009) doi:10.1103/PhysRevC.79.035203 [arXiv:0811.0739 [hep-ph]].

[30] M. Bashkanov and H. Clement, Eur. Phys. J. A **50**, 107 (2014)

[31] G. Agakishiev *et al.* [HADES Collaboration], Eur. Phys. J. A **48**, 64 (2012)

[32] G. Agakishiev *et al.*, Eur. Phys. J. A **50**, 82 (2014)

[33] S. Teis et al., Z. Phys. A bf 356, 421 (1997).

[34] M. Zetenyi and G. Wolf, Heavy Ion Phys. **17**, 27 (2003) doi:10.1556/APH.17.2003.1.5 [nucl-th/0202047].

[35] J. Adamczewski-Musch *et al.* [HADES Collaboration], Eur. Phys. J. A **53**, no. 9, 188 (2017).

[36] J.Diaz *et al.*, Nucl. Instrum. Meth. A **478**, 511 (2002). doi:10.1016/S0168-9002(01)00895-6

[37] J. Adamczewski-Musch *et al.* [HADES], Phys. Rev. C **102** (2020) no.2, 024001 doi:10.1103/PhysRevC.102.024001 [arXiv:2004.08265 [nucl-ex]].

[38] R. Lalik [HADES Collaboration], J. Phys. Conf. Ser. **1137** (2019) no.1, 012057. doi:10.1088/1742-6596/1137/1/012057